**THE EUROPEAN
PHYSICAL JOURNAL B**

Microwave control of transport through a chaotic mesoscopic dot

T. Prosen[1] and D.L. Shepelyansky[2,a]

[1] Physics Department, Faculty of Mathematics and Physics, University of Ljubljana, Ljubljana, Slovenia
[2] Laboratoire de Physique Théorique, UMR 5152 du CNRS, Univ. P. Sabatier, 31062 Toulouse Cedex 4, France

Abstract. We establish analogy between a microwave ionization of Rydberg atoms and a charge transport through a chaotic quantum dot induced by a monochromatic field in a regime with a potential barrier between dot contacts. We show that the quantum coherence leads to dynamical localization of electron excitation in energy so that only a finite number of photons is absorbed inside the dot. The theory developed determines the dependence of localization length on dot and microwave parameters showing that the microwave power can switch the dot between metallic and insulating regimes.

PACS. 05.45.Mt Quantum chaos; semiclassical methods – 73.50.Pz Photoconduction and photovoltaic effects – 32.80.Rm Multiphoton ionization and excitation to highly excited states (e.g., Rydberg states)

The dynamical localization of quantum chaos is a generic physical phenomenon induced by quantum coherence which leads to suppression of diffusive wave packet spreading originated from dynamical chaos in the classical limit (see e.g. [1] and Refs. therein). It has been first seen in numerical simulations of the kicked rotator model [2] and, later, of a more realistic system of excited hydrogen atom in a microwave field [3]. The first observation of this phenomenon was achieved in microwave ionization experiments of hydrogen and Rydberg atoms [4–7] while more recent experimental progress allowed to realize the original kicked rotator model with cold atoms in laser fields and detect with them the dynamical localization of chaos [8].

For a hydrogen atom in a microwave field the diffusive excitation in energy appears only above certain field threshold where the integrability of unperturbed motion is destroyed and the classical dynamics becomes chaotic [9]. However, in certain systems the internal dynamics can be almost fully chaotic on an energy surface so that classically the diffusive excitation starts for arbitrary small fields. As an example of such systems we may quote complex molecules [10], Rydberg atoms in a magnetic field [11] or chaotic Sinai billiards [12]. In such systems the quantum eigenstates are chaotic and their level spacing statistics is described by the random matrix theory [10,11,13,14]. The excitation of such quantum systems by a monochromatic field represents a diffusive process of one-photon absorption/emission transitions with a rate Γ which is given by the Fermi golden rule. The quantum interference effects

a URL : http://www.lpt.irsamc.ups-tlse.fr/~dima

lead to the dynamical localization of this diffusion with the localization length l_ϕ given by [15]:

$$l_\phi = 2\pi\hbar\Gamma\rho_c . \tag{1}$$

Here l_ϕ is measured in the number of photons of monochromatic field with frequency ω, ρ_c is the level density of unperturbed system and it is assumed that $\hbar\omega\rho_c > 1$ and $l_\phi > 1$. The extensive numerical simulations of a microwave ionization of internally chaotic Rydberg atoms (chaos is produced by static magnetic or electric field) [16] showed that the relation (1) works even in extreme regimes when up to a thousand of photons is needed to ionize one atom.

The result (1) is rather general and can be used not only for atoms but also for chaotic billiards in a microwave field. In fact, during the last decade the conductance properties of such billiards realized with 2D electron gas quantum dots of micron size have been studied in great detail both experimentally and theoretically (see reviews [17,18] and Refs. therein). In such experiments typical parameters correspond to a dot size $a \sim 1\,\mu$m and electron density $n_e \sim 4 \times 10^{11}\,$cm^{-2}. With the spin degeneracy the level number at the Fermi energy is $n_F = n_e\mathcal{A}/2 \approx 2000$ where the dot area is $\mathcal{A} \sim a^2$. These values of a and n_F correspond to those of a Rydberg atom with the principal number $n \sim 100$. Indeed, the atom size is $a \sim n^2 a_B \sim 0.5\,\mu$m and the level number, inside a set with fixed magnetic quantum number $m_z \sim 1$, is $n_F \approx n^2/2 \sim 5000$ (see e.g. [16]). Here a_B is the Bohr radius and m_z is preserved for a linearly polarized field. Thus, a quantum dot with the above parameters can be viewed as a mesoscopic
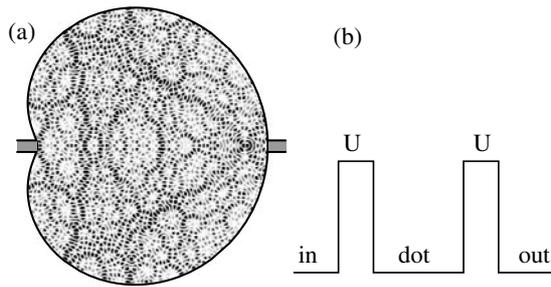
Fig. 1. (a) Dot billiard at $\lambda = 3/8$ with the probability density of the eigenstate at the Fermi level $n_F = 2001$ (see text); density is proportional to grayness. Dashed stripes show schematically income (left) and outcome (right) leads. (b) Sketch of tunneling barriers of height U between income lead, dot and outcome lead .

"Rydberg" atom. A tunneling barrier of height U between the dot and the income/outcome lead (see Fig. 1) creates an effective ionization potential similar to the one of Rydberg atom. The in/out direction is determined by a small applied voltage driving electrons from left to right (Fig. 1b). The microwave field will switch the dot conductance from insulating ($\hbar\omega l_\phi \ll U$) to metallic ($\hbar\omega l_\phi > U$) regime. The structure with one dot can be repeated few times consecutively along one direction to enhance the current signal variation with system parameters.

To understand in a better way the requirements for microwave parameters we note that for the 2D electron gas the Fermi momentum p_F and energy E_F are given by $p_F^2 = 2\pi n_e \hbar^2$ and $E_F = p_F^2/2m$ with $m = 0.067m_e$ for nGaAs. The average level spacing in the dot is $\Delta = 1/\rho_c = E_F/n_F = 2\pi\hbar^2/m\mathcal{A}$. For the typical values of a and n_e used above we obtain $E_F \sim 100$ K, $\Delta \sim 0.05$ K with the Fermi velocity $v_F = p_F/m \sim 2 \cdot 10^7$cm/s. Hence, the collision frequency is $\nu_c/2\pi = v_F/2a \sim 100$ GHz that is much larger than the frequency corresponding to one level spacing $\Delta/(2\pi\hbar) \sim 1$ GHz. Thus for a microwave field with $\omega/2\pi < 100$ GHz ac-driving is in the classical adiabatic regime and according to the adiabatic theorem the energy excitation is exponentially small for dot billiards with integrable dynamics. However, for dots with chaotic dynamics a microwave field with $\hbar\omega > \Delta$ leads to diffusive excitation in energy E with the rate $D_E = (\delta E)^2/\delta t \approx \hbar^2\omega^2\Gamma$. In analogy with a chaotic atom [16] in a linearly x-polarized field we have $\partial E/\partial t = \epsilon\omega x \cos\omega t$ and $D_E \sim (\epsilon a\omega)^2/\nu_c$ where ϵ is the field strength multiplied by the electron charge. This gives

$$l_\phi \approx 2\pi\chi\epsilon^2 a^2/(\hbar\nu_c\Delta) \approx 16\chi\epsilon^2(\mathcal{A}/\mathcal{A}_0)^{5/2}(n_{e0}/n_e)^{1/2} \quad (2)$$

where χ is a numerical constant and in the right part $\mathcal{A}_0 = 1\,\mu m^2$, $n_{e0} = 4 \times 10^{11}$ cm^{-2} and ϵ is measured in V/cm. It is also convenient to write (2) in the form $l_\phi \approx \chi(\epsilon a/E_F)^2 n_F^{3/2}$ which shows that l_ϕ may be large even when $\epsilon a \ll E_F$.

To check the validity of the above estimates and obtain all numerical coefficients we study numerically the dynamical photonic localization in the billiard which is given by a conformal quadratic map of a unit circle proposed by Robnik [19]. Its shape in polar coordinates is $r(\phi) = R(1 + 2\lambda\cos\phi)$ with a parameter $\lambda \in [0, 1/2]$. For $\lambda > 1/4$ the billiard is non-convex and almost fully chaotic, while for $\lambda = 1/2$ it is rigorously known to be ergodic and belongs to the class of K-systems [12]. We restrict our studies mainly to the case with $\lambda = 3/8$ shown in Figure 1. For the quantum evolution we consider only even states of the billiard. These states are symmetric with respect to reflection transformation y to $-y$ and a microwave field linearly polarized along x-axis gives transitions only inside this symmetry class. We take the Fermi level to be $n_F = 2001$ in this symmetry class (total quantum number around 4000) that corresponds to $E_F = v_F^2/4 = 12586.2$ where for numerical simulations we use the usual billiard units with $\hbar = R = 2m = 1$. Then near E_F the average level spacing for this symmetry class is $\Delta = 6.266$. The numerical method introduced in [19] allows to find efficiently the billiard eigenstates and the dipole matrix elements between them (the eigenstate at the Fermi level is shown in Fig. 1). Therefore, the quantum evolution induced by a microwave field can be numerically integrated directly in the eigenbasis. This approach allows to follow the quantum excitation over thousands of microwave periods. The integration time step was set to $\Delta t = 10^{-4}$ and we ensured that its modification did not affect the excitation probabilities. In the numerical simulations the transitions below n_F were suppressed, since in a dot all states below n_F are occupied by electrons, and up to $n_{tot} = 2000$ levels above n_F were taken into account. The escape in outcome lead is modeled as absorption of all probability above the level number $n_F + n_I$ after a microwave pulse of finite duration. This corresponds to the tunneling barrier height $U = n_I\Delta$ between the dot and outcome lead.

Examples of probability distribution w_n over billiard eigenstates n after a long microwave pulse are shown in Figure 2. They clearly show exponential localization of probability which can be approximately described by $w_n \sim \exp(-2n/l)/l$. The localization length in the basis n is related to the photonic length $l_\phi = l\Delta/\omega$. For large $\omega = 160$ the distribution shows a chain of equidistant peaks corresponding to one-photon transitions with the distance between peaks $\delta n = \omega/\Delta$. For $\omega \sim \Delta$ the peaks disappear and w_n decays in a homogeneous way.

The localization length l_ϕ can be expressed through the correlation function of dynamical motion inside the billiard. Indeed, as discussed in [20] in the semiclassical regime the dipole matrix elements of x can be expressed via the spectral density of dynamical variable $x(t)$. Using the definition of D_E and the expression for $\partial E/\partial t$ we obtain $D_E = \epsilon^2\omega^2 R^2 S(\omega/\omega_c)/2\omega_c$. Here $\omega_c = v_F/R$ and $S(\kappa) = \lim_{T\to\infty} \left|\int_{-T}^T d\tau\xi(\tau)e^{i\kappa\tau}\right|^2/2T$ is the dimensionless spectral density of $\xi(\tau) = x(t)/R$ with $\tau = \omega_c t$ and $\kappa = \omega/\omega_c$. Together with (1) this result leads to

$$l_\phi = \frac{\pi\epsilon^2 R^2}{\hbar\omega_c\Delta} S(\omega/\omega_c). \quad (3)$$
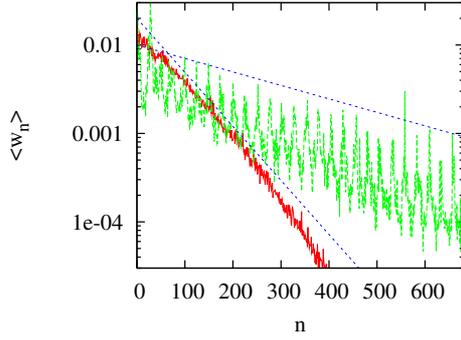
Fig. 2. (color online) Probability distribution $\langle w_n \rangle$ over the billiard eigenstates n after a pulse of 2000 microwave field periods (averaged over last 500 periods, n is counted from the Fermi level n_F). Here $\epsilon = 1200$, $\omega = 20$ (red/black curve) and $\epsilon = 300$, $\omega = 160$ (green/gray curve). Initially all probability is in the state $n = 0$ shown in Figure 1. The straight dotted lines show the theoretical exponential decay with the localization length (3).
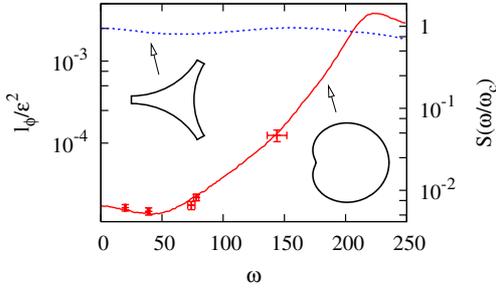

Fig. 3. (color online) Dependence of the scaled localization length l_ϕ/ϵ^2 (left axis) on the microwave frequency ω. Numerical data for $\epsilon = 1200, 1200, 1200, 600, 300$ (from left to right) are shown by points with error bars, the full curve shows the theory (3) with the classical spectral density $S(\omega/\omega_c)$ taken from [20] for the billiard of Figure 1 (sketch), here $\omega_c \approx 224$, $\Delta = 6.266$. Right axis shows the scale for $S(\omega/\omega_c)$. The dashed curve shows the classical spectral density $S(\omega/\omega_c)$ for the 3-disks billiard (sketch); ω is adjusted to the same collision frequency ω_c as for the full curve case.

In the billiard units $\omega_c = 2\sqrt{E_F}$ and for our value of E_F we have $\omega_c \approx 224$ and $l_\phi/\epsilon^2 \approx S/448$. The classical spectral density $S(\omega/\omega_c)$ has been found numerically in [20] and we show it in Figure 3. As it is seen, $S(\omega/\omega_c)$ has one maximum with $S(1) \approx 1.8$ and it goes to a constant value $S(0) \approx 0.004$ near zero. Using (3) we can determine the quantum localization length l_ϕ from the classical value of S. Without any fit parameters this relation gives a good agreement with the numerical data of Figure 2.

To check the theory (3) in more detail we determine the value of l_ϕ from the fit of exponential probability decay: $\langle w_n \rangle \propto \exp(-2n\Delta/\omega l_\phi)$ (w_n is integrated in one-photon interval to extract l_ϕ). The dependence of l_ϕ/ϵ^2 on ω is shown in Figure 3 demonstrating a good agreement with the theoretical formula (3) [21]. The dependence on ϵ at a fixed ω is shown in Figure 4. It is also in a good agreement with the theory (3) while $l_\phi \gg 1$ which is assumed by the semiclassical approach [22].
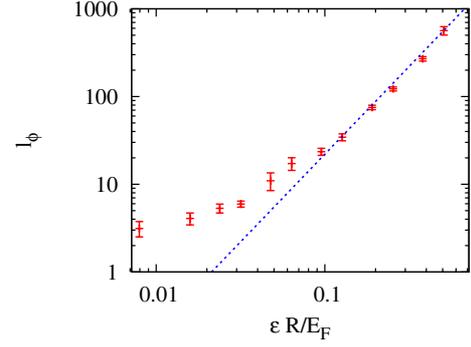

Fig. 4. (color online) Localization length l_ϕ as determined from numerical data (points) versus dimensionless field strength $\epsilon R/E_F$ for $\omega = 20$. The straight line gives the theoretical dependence (3).

The nontrivial property of equation (3) is that l_ϕ is directly dependent on the dynamical spectrum $S(\omega/\omega_c)$. For the mesoscopic billiards discussed above $\omega \ll \omega_c$ and it is interesting to have billiards with large value $S(0)$. Since $S(0)$ is simply the integrated auto-correlation function of $\xi(\tau)$, a possible choice is a billiard formed by three touching disks which exhibits a slow polynomial decay of correlations (see e.g. [23]). In Figure 3 we show the classical power spectrum $S(\omega/\omega_c)$ versus ω for the 3-disks billiard (see sketch, the opening between touching circles has a length $0.05R$). In this case the spectrum has a plateau at small ω that gives the value of $S(0)$ by a factor 250 larger compared to the billiard of Figure 1. The comparison of (3) with (2) gives $\chi = S(0)/4$ ($a = 2R$, $\nu_c = \pi\omega_c/2$). For the 3-disks billiard we have $\chi \approx 0.25$ and $l_\phi \approx 1$ for $\epsilon = 0.5V/cm$ and $\mathcal{A} = \mathcal{A}_0$, $n_e = n_{e0}$.

In fact the billiard shape is of primary importance for the efficiency of microwave excitation. Indeed, a decrease of λ from $\lambda = 3/8$ to $\lambda = 0.1$ makes the unperturbed dynamics inside the billiard quasi-integrable. In the latter case a microwave field acts in an adiabatic way and the current through the dot is reduced by orders of magnitude compared to the chaotic billiard as it is shown in Figure 5 [24]. This figure also shows that for a chaotic billiard the current through the dot is strongly reduced as soon as $\hbar\omega l_\phi$ becomes smaller than the barrier height $U = n_I \Delta$. Therefore, a conductance g between leads can be efficiently changed by varying a microwave field power. The conductance appears due to diffusion in energy which is rather similar to spatial diffusion in mesoscopic quasi-one-dimensional wires. Using analogy with the latter case where $g = E_c/\Delta$ [25], we can write the microwave conductance of the billiard as

$$g \sim l_\phi \exp(-2N_I/l_\phi)/N_I, \tag{4}$$

where $E_c = \hbar D_E/U^2$ is the Thouless energy for diffusion in energy space, $N_I = U/\hbar\omega$ is the number of photons required to pass over the lead barrier U and an effective level spacing between quasienergy levels is $\Delta_{ef} \sim \Delta/N_I$. As in [25] it drops with the sample size N_I and $g \sim E_c/\Delta_{ef}$. For $l_\phi \gg N_I$ the dot is in the metallic regime while for $l_\phi \ll N_I$ it is insulating. Thus a microwave field can
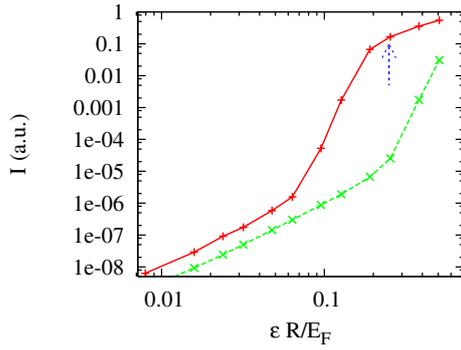
Fig. 5. (color online) Dependence of the current I through a dot billiard on a scaled microwave field strength $\epsilon R/E_F$ at $\omega = 20$, $n_F = 2001$. The current I, shown in arbitrary units, is determined as the probability on billiard eigenstates, within $2500 \leq n \leq 4000$, absorbed after a field pulse of 2000 microwave periods duration. Two curves correspond to fully chaotic billiard at $\lambda = 3/8$ (top) and to quasi-integrable billiard at $\lambda = 0.1$ (bottom). The arrow marks the position where the absorption border is reached by localization $n_I = 500 = \hbar \omega l_\phi / \Delta$.

efficiently switch on and off the conductance of a chaotic quantum dot blocked by a tunneling barrier U between the dot and outcome lead. To distinguish clearly the dependence (4) from the Arrhenius activation law at finite temperature T we need to have $T \ll \hbar \omega l_\phi$.

Of course, above we used a rather simplified model neglecting interactions between excited electrons and finite temperature of a dot. These effects destroy quantum coherence and dynamical localization and should be taken into account when comparing the theory with the experiment. However, we expect that a transition from metallic to insulating behavior induced by a microwave field (see (4)) is a robust phenomenon and thus it can be observed experimentally as it has happen with a microwave ionization of Rydberg atoms. Present experimental techniques allow to observe effects of microwave radiation on electron transport in mesoscopic dots (see e.g. [26,27]) that makes possible experimental investigations of the effects discussed here.

References

1. B.V. Chirikov, in *Chaos and Quantum Physics*, Les Houches Lecture Series **52**, edited by M.-J. Giannoni, A. Voros, J. Zinn-Justin (North-Holland, Amsterdam, 1991), p. 443

2. G. Casati, B.V. Chirikov, J. Ford, F.M. Izrailev, Lecture Notes in Physics **93**, 334 (1979)

3. D.L. Shepelyansky, preprint Inst. of Nucl. Phys. N. 83-61 (Novosibirsk, 1983); G. Casati, B.V. Chirikov, D.L. Shepelyansky, Phys. Rev. Lett. **53**, 2525 (1984)

4. E.J. Galvez, B.E. Sauer, L. Moorman, P.M. Koch, D. Richards, Phys. Rev. Lett. **61**, 2011 (1988)

5. J.E. Bayfield, G. Casati, I. Guarneri, D.W. Sokol, Phys. Rev. Lett. **63**, 364 (1989)

6. M. Arndt, A. Buchleitner, R.N. Mantegna, H. Walther, Phys. Rev. Lett. **67**, 2435 (1991)

7. H. Maeda, T.F. Gallagher, Phys. Rev. Lett. **93**, 193002 (2004)

8. F.L. Moore, J.C. Robinson, C.F. Bharucha, B. Sundaram, M.G. Raizen, Phys. Rev. Lett. **75**, 4598 (1995)

9. N.B. Delone, V.P. Krainov, D.L. Shepelyansky, Sov. Phys. Uspekhy **26**, 551 (1983)

10. Th. Zimmermann, L.S. Cederbaum, H.-D. Meyer, H. Köppel, J. Phys. Chem. **91**, 4446 (1987)

11. H. Friedrich, D. Wintgen, Phys. Rep. **1983**, 37 (1989)

12. I.P. Kornfeld, S.V. Fomin, Ya. G. Sinai, *Ergodic theory* (Springer, Berlin, 1982)

13. O. Bohigas, M.J. Giannoni, C. Schmit, Phys. Rev. Lett. **52**, 1 (1984)

14. M.V. Berry, M. Robnik, J. Phys. A **19**, 1365 (1986)

15. D. Shepelyansky, Physica D **28**, 103 (1987)

16. G. Benenti, G. Casati, D.L. Shepelyansky, Eur. Phys. J. D **5**, 311 (1999)

17. C.W.J. Beenakker, Rev. Mod. Phys. **69**, 731 (1997)

18. Y. Alhassid, Rev. Mod. Phys. **72**, 895 (2000)

19. M. Robnik, J. Phys. A **16**, 3971 (1983); M. Robnik, J. Phys. A **17**, 1049 (1984)

20. T. Prosen, M. Robnik, J. Phys. A **26**, L319 (1993); T. Prosen, Ann. Phys. (NY) **235**, 115 (1994)

21. Equation (3) assumes that the energy excitation $\hbar \omega l_\phi$ remains small compared to E_F, at large ω it gives a noticeable fraction of E_F that leads to horizontal error bars in Figure 3

22. Also the size of field oscillations should be larger than the wavelength implying $\epsilon/(m\omega^2) > R/n_F^{1/2}$

23. R. Artuso, G. Casati, I. Guarneri, Phys. Rev. E **51**, R3807 (1995)

24. While in experiments it may be not easy to vary directly a dot shape, it may be possible to introduce a magnetic field which should make the dynamics quasi-integrable as soon as the Larmor radius becomes much smaller than the dot size. For a dot with parameters $\mathcal{A}_0$ and n_{e0} discussed above this corresponds to a magnetic field $B \sim 1$ T

25. D.J. Thouless, Phys. Rev. Lett. **39**, 1167 (1977)

26. A.A. Bykov, G.M. Gusev, Z.D. Kvon, D.I. Lubyshev, V.P. Migal', JETP Lett. **49**, 13 (1989)

27. R. Deblock, Y. Noat, B. Reulet, H. Bouchiat, D. Mailly, Phys. Rev. B **65**, 075301 (2002)